Sādhanā (2023)48:6
https://doi.org/10.1007/s12046-022-02053-4

Flow regimes of submerged rectangular sharp-crested weirs in sand bed channel

SAEED SALEHI[1,2], AMIN MAHMUDI MOGHADAM[3,*] and KAZEM ESMAILI[4]

[1]Department of Civil Engineering, Lakehead University, Thunder Bay, ON P7B 5E1, Canada
[2]Department of Agriculture Engineering, Ferdowsi University of Mashhad, Mashhad, Iran
[3]Faculty of Civil Engineering Department, Shams Institute of Higher Education, Golestan Province, Gonbad, Iran
[4]Department of Civil Engineering, Ferdowsi University of Mashhad, Mashhad, Iran
e-mail: Ssalehi@lakeheadu.ca; saeedsalehi100@gmail.com; amin.mahmudi@modares.ac.ir; eesmaili@gmail.com

MS received 29 July 2020; revised 15 May 2022; accepted 4 October 2022

Abstract. Laboratory experiments were conducted out to investigate the regimes of submerged flows over the sharp-crested weirs in sand bed Channel. These kinds of flows were classified as five states such as (I) impinging jet, (II) bed surface flow, (III) surface jump, (IV) surface wave, and (V) surface jet based on the depicted vector plots of the regimes. By increasing the submergence ratio, the impinging jet was developed as a downward jet which was impinged from the weir crest to the downstream. By continue the increasing, flow regime was developed as a bed-surface flow which is supposed that the impinging jet is turned as flow near the bed position instead of having a direct impact with the bed. Additionally, increasing constancy of the submergence ratio causes that the bed-surface regime turned to the surface jump which is accompanied by a hydraulic jump at the water surface. Subcritical condition at downstream of the weir which is provided by raising the tailwater due to constant flow discharge causes that the surface wave regime has vanished at the water surface of the downstream of the weir and some oscillating waves were transferred to downstream. Finally, by considering the maximum range of submergence ratio, the flow regime was changed to the surface jet which was accompanied by a big clockwise vortex at the lower water elevation. The present study classifies these flow regimes based on the velocity components (u, v, w). This approach was chosen by the authors to show the different classification between visual inspection and investigating the velocity direction by ADV. Then, an empirical equation was proposed to show the boundaries of the presented regimes. Also, a dynamic restriction was proposed based on experimental and literate data as a non-eroded status that is due to a submerge ratio, the scour hole is not provided at downstream of sharp-crested weir.

Keywords. Discharge; flow regime; submerged flow; sharp-crested weirs; sediment transport.

1. Introduction

Sharp-crested weirs have many applications in civil and environmental engineering for flow measurement, water level control in irrigation channels, and also increasing the storage capacity of reservoirs [1]. If the downstream water level of a weir is lower than the weir crest, the flow over the weir is regarded as free flow condition. But if the downstream water level above the weir crest, the flow is considered as submerged condition. At the onset of flow submergence (i.e., modular limit), the upstream water level h is affected by the tailwater and rises. Where the tailwater is higher than weir crest, the flow over the weir is dependent on both of water head at the upstream and downstream the weir. During the increasing water level at the downstream the weir, the flow condition is changed from free flow to submerged flow. Many researchers on the flow patterns over the weirs between free and fully submerged flow based on the submergence ratio t/h to impinging jet, surface jet, and surface wave regimes have classified [2–6]. These were mainly employed for the visual inspection. It seems that the flow characteristics are dependent on the flow regimes pattern which directly effects on sediment erosion at downstream and upstream the sharp crested weir SCW [7].

According to Wu and Rajaratnam, for a certain discharge, as a ratio, t/h, is increased so the submerged-flow over the weir passes through several regimes. Submerged flow was divided into four regimes; (I) impinging jet, (II) surface jump flow, (III) surface wave, (IV) surface jet. It assumes that this classification was presented based on

*For correspondence
Published online: 27 December 2022

visual inspection which indicated for the impinging jet regime, the flow over the weir plunges into the tailwater. This regime diffuses as a plane submerged jet, and eventually hits the bed of the downstream channel. For the surface flow regime, the flow remains as a downstream surface jet, and the scour hole downstream of the weir is made by the increasing jet thickness and turbulence mixing with the tailwater; however, for the IJR, the scour hole downstream of weir is induced by the direct impact of the plunging jet over the weir [2].

Guan *et al* proposed an index (α) ($\alpha = (u_a/u_c)\ (z/h_t)^{0.2} = 1.45$), where u_a is average approach flow velocity, u_c is critical approach flow velocity and z/h_t is the ratio between weir height and tailwater depth), by increasing index *a* flow regime changes from impinging jet to surface regime. It shows that the submergence ratio directly effects on flow patterns and it can be proposed by considering Froude number restriction at the downstream of submerged SCW. Furthermore, they proposed four regimes as: (1) A-jump; (2) plunging jet; (3) surface waves; and (4) surface jet. Also, they investigated the scour hole formation around a sharp-crested weir in live-bed sediment flow and deeply submerged flow conditions. It was reported that the flow regimes over the weir were independent of the sediment size. A new equation was proposed to better express the boundary of the transient regime between impinging and surface jet regimes [7].

The impinging jet flow and surface flow regimes for the first time were divided by considering the submerged ratio and then by considering visual inspection based on hydraulic parameter [8]. Also, flow forms were investigated into a surface jet over a longitudinal distance of 2t and it behaves like a turbulent surface [9].

Figure 1 shows the schematic of the presented regimes. Figure 1a) shows the surface jet regime, figure 1b) is the surface wave regime, figure 1c) is the surface jump flow and figure 1d) is allocated to impinging jet.

Many studies conducted to predict the score hole depth at the downstream submerged sharp crested weir by considering the flow regimes approach and many empirical equations have been proposed based on the hydraulic characteristics [10–23]. There are still a few researches which were carried out on turbulence structure and flow pattern at the submerged sharp crested weir by monitoring and evaluation of the flow patterns. Guan *et al* investigated the distribution of time-averaged velocity vectors on the centerline longitudinal section of the experimental channel. The velocity vectors were depicted from the average values of the stream-wise and vertical velocity components by considering the vector addition. Results show that upstream flow was quite uniform even at the equilibrium stage. When this uniform flow approaches near the submerged weir, the flow pattern is altered by the sudden change of bed elevation. The approach flow is accelerated at the crest of the weir and a weak back flow was created immediately at the upstream of the weir. The downstream of the submerged weir were divided into two zones such as recirculation zone and flow reattachment region. Also, by calculating velocity components, turbulence kinetic energy and Reynolds shear stress was calculated within a longitude section. The turbulence structured ahead of the recirculation zone formed the dimensions of the scour hole [24].

The past studies by Wu and Rajaratnam [2] and [3]; Azimi *et al* [6]; and Guan *et al* [7] were carried out by considering visual inspections rather than to plot flow patterns by ADV measurement or other approaches. Lack of employing new experimental probes like ADV and PIV can be considered as a new approach for classifying the flow regimes over the sharp crested weirs which is assumed that has much accuracy for proposing the boundaries of the developed flow regimes. Also, classifying the flow over the hydraulic structure by employing the new experimental probes can illustrate the flow currents due to the different regimes which were not provided based on visual inspection approach. Therefore, present study has been carried out to plot and present the developed regimes at the downstream of submerged weir by employing the patterns of

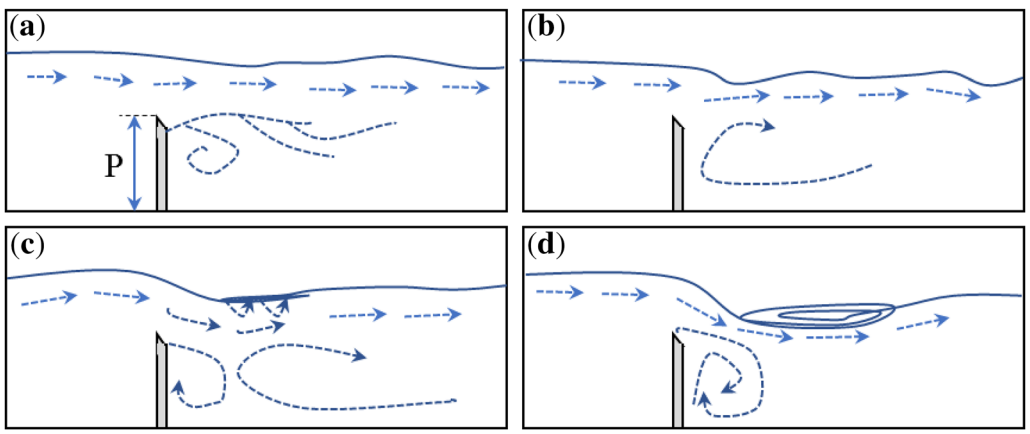

Figure 1. The flow regimes over the sharp-crested weir in submergence condition.

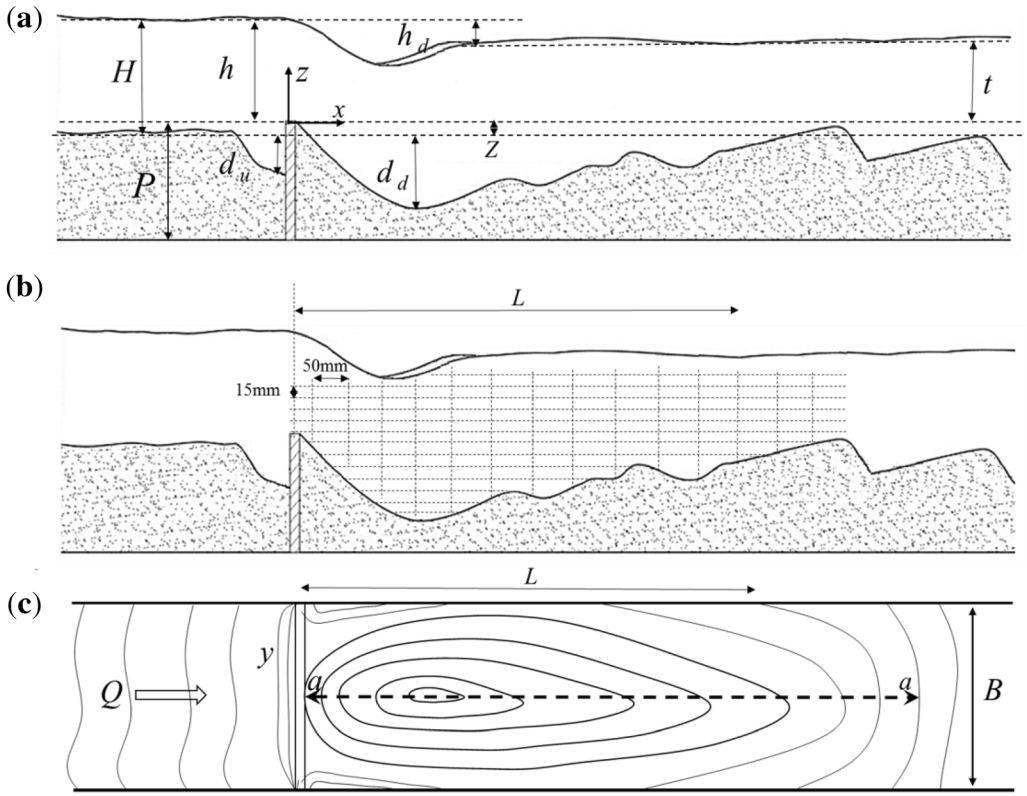

Figure 2. Scheme of experimental setup and adopted coordinate system; (a) side view (x–z) plan, (b) ADV grid plan and (c) top view (x–y) plan.

flow vectors which were collected by ADV probe. It is predicted that decreasing submerged ratio changes flow regime from surface jet to a big clockwise vortex based on previous researches [2, 24], but it seems that for a given discharge, as a ratio, t/h, is decreased, during the impinging jet regime is formed to the surface jet regime, the new flow pattern has emerged along this transformed process (i.e., raising the submergence ratio). It is supposed that the new developed regime is neither imping jet flow patterns nor the surface jump regime. The new regime is proposed as a bed-surface regime which has a behavior same as surface jump accompanied by the underflow near the bed. It seems that the sediment deposition is dramatically increased during this bed-surface flow. So, the present study classifies the flow regime over the sharp-crested weir and proposes its boundary by using ADV measurement.

2. Experimental setup

The experiments were conducted within a horizontal, rectangular, glass-walled flume 10 m long, 0.61 m wide, and 0.50 m high in the hydraulic laboratory of Lakehead University. To measure and calibrating the flow discharge of the experimental channel, a triangular weir was adjusted at the flume entrance. Also, a screen was installed at the entrance of channel to reduce the surface water fluctuations and develop a steady uniform flow. The bed elevation at the initial and end of the channel was brought up to 250 mm by installing wooden plates to provide a box for embanking sediment and locating the sharp-crested weir. The length of this stage was 3 m as it can be seen at figure 2a). The upstream and downstream of the weir filled by sand d_{50}=1.1 mm. The sharp-crested weir thickness was about 6 mm which was fabricated through the considered sandbox. Two Piezometer were installed to measure the water level at 0.5 m upstream and downstream of the weir models. Flow rates Q were measured using an inline magnetic flow meter with an accuracy of ±0.01 L/s (FMG 600, Omega, Canada). Also, discharges were measured by the triangular weir. The accuracy of the magnetic flow meter was tested with volumetric discharge measurements, too. Variations in discharge during the experiments were within ±0.3% to ±1% of the average in low and high flows respectively. One sharp-crested weir was installed through the sediment stage with weir height of P=0.03 m. To evaluate flow patterns at the downstream sharp-crested weir, in total, 24 laboratory experiments were conducted by considering the different submergence ratios and flow discharge (see table 1). The discharge range was from 3.9 L/s to 17.7 L/s as it can be seen in table 1. It should be mentioned that the experimental set up were deduced from Guan's experiments in

Table 1. Results of experimental tests of submerged sharp-crested weir.

No. 1	Q (L/s)	t (mm)	h (mm)	t/h_o	z (mm)	h_d (mm)	d_{md} (mm)	u_{ave}/u_c	λ
1	3.95	31	40	0.78	30	9	0	0.24	4.59
2	3.95	20	37	0.54	30	17	22	0.32	5.01
3	3.95	13	36	0.36	30	23	75	0.40	5.82
4	3.95	5	36	0.14	30	31	185	0.59	7.24
5	3.95	−7	36	−0.19	30	43	187	0.82	9.24
6	6.49	69	75	0.92	30	6	0	0.21	2.71
7	6.49	56	68	0.82	30	12	0	0.26	3.42
8	6.49	40	57	0.70	30	17	0	0.33	3.45
9	6.49	33	54	0.61	30	21	0	0.38	3.54
10	6.49	30	54	0.56	30	24	152	0.41	3.65
11	6.49	24	52	0.46	30	28	167	0.47	3.65
12	6.49	17	52	0.33	30	35	192	0.57	3.69
13	9.42	92	95	0.97	30	3	0	0.24	1.58
14	9.42	70	78	0.90	30	8	0	0.31	2.18
15	9.42	55	71	0.77	30	16	0	0.38	2.69
16	9.42	44	67	0.66	30	23	85	0.45	2.89
17	9.42	34	67	0.51	30	33	122	0.54	3.09
18	9.42	26	67	0.39	30	41	162	0.65	3.12
19	17.77	121	129	0.94	30	8	0	0.35	1.64
20	17.77	102	112	0.91	30	1	0	0.41	1.63
21	17.77	82	111	0.74	30	29	0	0.50	2.42
22	17.77	76	110	0.69	30	34	138	0.54	2.50
23	17.77	70	109	0.58	30	39	152	0.58	2.55
24	17.77	55	103	0.53	30	48	228	0.71	2.47

order to make comparison between the presented flow regimes.

Detailed hydraulic, sediment transport tests and water surface level were conducted to study the structure of three-dimensional flow, turbulence, and bed scour formation downstream of submerged sharp-crested weirs. Due to a mount of flowed discharge over the weir, the submergence ratio was decreasing by sluice gate at the downstream the flume from $t/h \approx 1$ to free flow. As it expected, due to special t/h the scour profiles developed at the bed position (t is the different water level between upstream and downstream weir and h is total head over the weir crest). It seems that the surface jet was transformed to surface jump and then the depleted jet was plunged to the bed surface. During this process, within the different submergence ratio velocity components were measured by ADV probe. The instantaneous three-dimensional water velocity components were measured along longitudinal x, transverse y, and vertical z directions. Figure 2a presents the hydraulic and geometry on this current research.

By stabilizing the bed surface and equilibrium condition the velocity was measured based on the gridded surfaces upstream of the weirs (see figure 2b) show the locations of velocity component measurements by the ADV probe (Vectrino, Nortek AS, Norway). It should be mentioned that the measurement process were commenced after the equilibrium condition which was attained around 4-6 hours from the begging of the tests. By increasing the submergence ratio, the time exceeds around 7 hours. To assure of equilibrium condition, the maximum scour hole was measured constantly and due to a decrease in the variation the velocity measurement process has been started by employing the ADV probe. To prevent the scour hole by ADV probe, the ADV sensor were located 50 mm above the bed. By this approach the sudden agitation was confined above the bed region and the scour hole formation did not vary.

The critical threshold velocity was calculated based on assuming a logarithmic velocity profile [i.e., $u_{ave}/u_{*c} = 5.75 \log (5.53h_o/d_{50})$] and shear velocities were determined from an approximated formula based on the Shields diagram (Melville 1997). All scour tests were commenced from an initial flatbed and continued until the equilibrium stage was achieved. Turbulence characteristics such as flow patterns, stream-wise velocity was extracted from velocity data after filtering the raw data in WinADV software. Filtering can be used to remove samples with low correlation scores or signal-to-noise ratios. Filtering may be based either on the 3-beam averages or the 3-beam minimums (2-beam averages and minimums for 2D probes). Samples tagged with communications error flags (999's) may also be removed (this error can only occur with field-model probes). Filtering based on velocity may be useful for removing samples that were aliased due to exceeding the velocity range

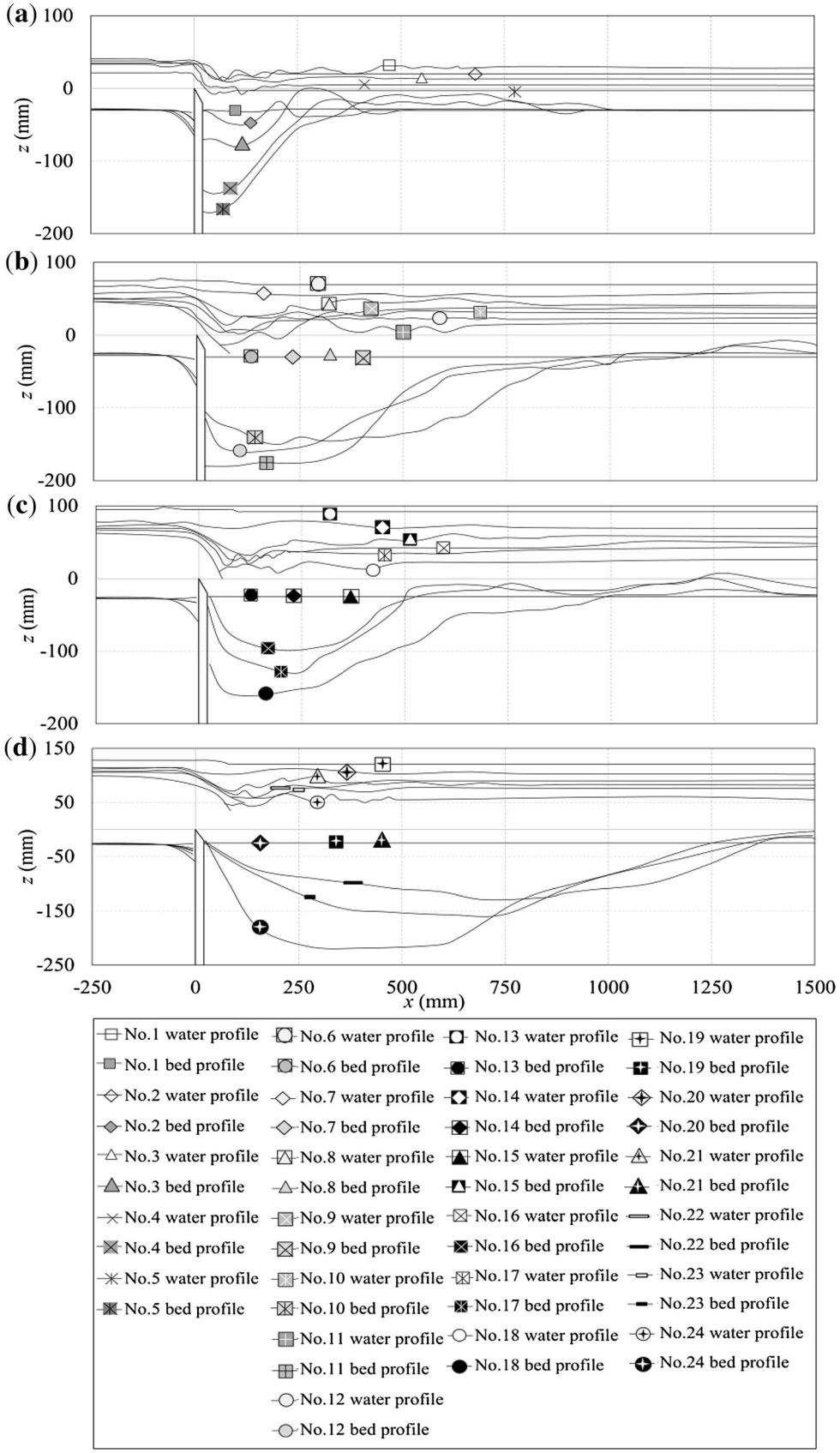

Figure 3. Scour profiles; (a) Q= 3.95 L/s, (b) Q = 6.49 L/s, (c) Q = 9.42 L/s, Q= 17.77 L/s.

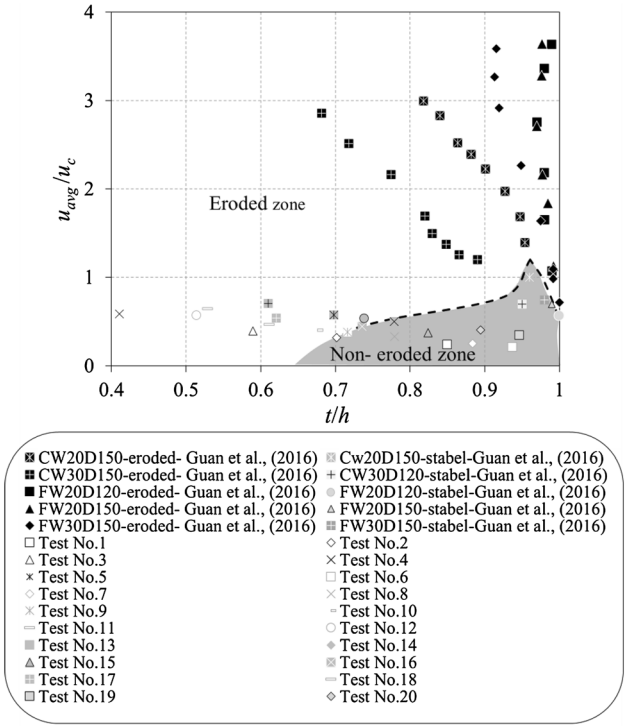

Figure 4. Non-eroded zone at the submerged weir.

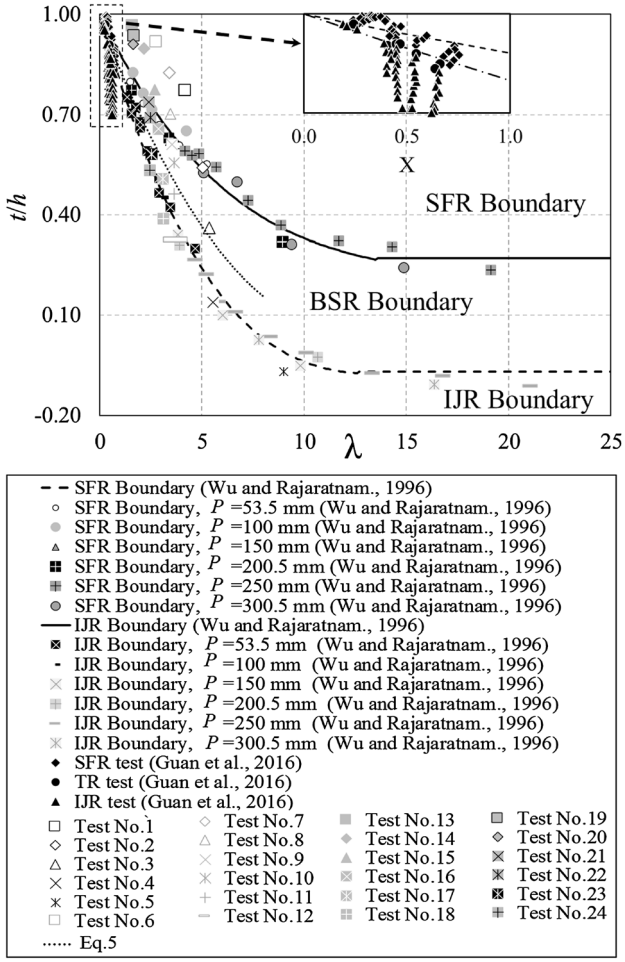

Figure 5. Bed-surface regime (BSR).

chosen at the time of data collection (velocity ambiguities). However, even with aliased samples removed, one must recognize that the data set is still biased by the absence of what should have been high-velocity data. In total, a sampling duration of 120 seconds with a sampling frequency of 200 Hz was selected for velocity measurements. To obtain high-quality measurements, the data series were filtered by considering, signal-to-noise ratio above SNR (dB)>15 and correlation coefficient above CORR>70%. All noises in time series data were filtered using circular-block bootstrap de-spiking techniques [25–31].

Some Laboratory experiments were carried out by Guan *et al* to measure the mean flow and turbulence at the downstream of the rectangular sharp-crested weirs in the live bed condition. In order to measure the velocity components, the Acoustic Doppler Velocimetr (ADV) technique was employed experimentally. A strong variation of the secondary currents was observed at the maximum score hole section at the downstream sharp-crested weirs. It was found that the turbulent intensity weirs were approximately governed by the formation of the scour hole; however, the flow pattern is still vague that how it has changed the flow vectors over the different flow regimes. Hence, experiments were performed to achieve this goal. Although some researches were carried out and proposed some regimes in submerged sharp-crested weir, but there is no research to show the flow patterns and flow direction through the divided regimes based on detailed hydraulic parameters.

3. Results and discussion

3.1 *Scour profiles*

Figure 3 shows the scour profiles and water surfaces along the longitudinal section of the submerged sharp-crested weir. These profiles were depicted from experimental measurements which were calculated by point gage along a longitudinal section (a–a) at the centerline of experimental flume. The values of the measured scour hole depths were reported in table 1. As it can be seen, figure 3 was divided as per bed-plots which are considered for four discharges as 3.95, 6.49, 9.45 and 17.77 L/s from a to d, respectively. The ratios u_{ave}/u_c were calculated based on laboratory parameters for 24 model. The variation of submergence ratio (i.e -0.2< t/h<0.97), u_{ave}/u_c values were less than one. It supposed that, the scour profiles were fixed and the erosion process did not happen at the special submergence ratio. In order to find the hydraulic boundary of non-erosion zone and eroded zone, the eroded profiles and non-eroded profiles were presented in figure 4. Additionally, the Guan's

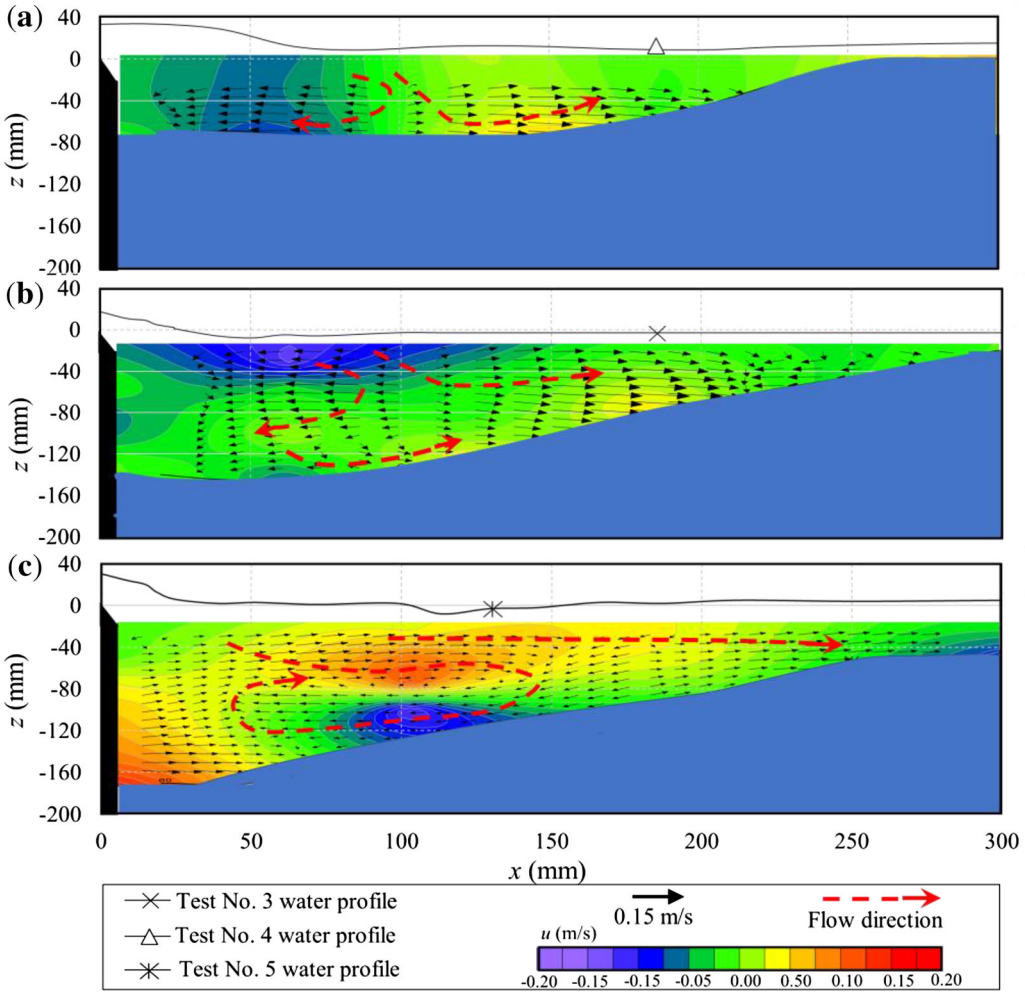

Figure 6. Flow regimes at the submerged weir; (a) Impinging regime of Model No. 3, (b) BSR (bed-surface regime) of Model No. 4, (c) Surface jump regime of Model No. 5.

experiments have been extracted from literature (Guan *et al* 2015). Based on some Guan's experiments, some scour profiles were not developed and the sandbed remained flat. This situation was considered as non-erosion zone which can be defined based on detailed hydraulic parameters (i.e., x/h and $u_{ave}/u_{c)}$. The proposed equations (1) and (2) based on experiments show that the zone in which the erosion will never happen (non-erosion zone, see figure 4). These boundaries were showed in figure 4. With all values of $u_{ave}/u_c>1$, the live bed channel condition is provided. In experimental test, as it can be seen, approximately $u_{ave}/u_c>0.5$ the bed is getting to eroded. Also, table 1 shows the values of the u_{ave}/u_c with t/h. It seems that the plunged jet at downstream gradually creates a scouring cavity. This process continues until it is stable between 5 and 21 hours.

$$\frac{u_{avg}}{u_c} = 1.32\left(\frac{t}{h_o}\right)^{4.72},\ 0.7 < \frac{t}{h_o} < 0.93 \rightarrow R^2 = 0.89 \quad (1)$$

Also, for $0.93<t/h_o<1$, this zone is defined as Eq. (2)

$$\frac{u_{avg}}{u_c} = 0.57\left(\frac{t}{h_o}\right)^{-19.4},\ 0.93 < \frac{t}{h_o} < 1 \rightarrow R^2 = 0.91 \quad (2)$$

3.2 *Developed regime*

Wu and Rajaratnam [2] has defined some boundaries for impinging jet regime based on their experiments and visual inspections. Based on their achievements, for λ in range of zero to 15 the boundaries are presented as follows:

$$\frac{t}{h_o} = 1 - 0.215\lambda + 0.0142\lambda^2 - 0.00031\lambda^3,\ (R^2 = 0.92) \quad (3)$$

where for λ greater than about 15, (t/h_o) = -0.07, and surface wave regime boundary were described as Eq. (4)

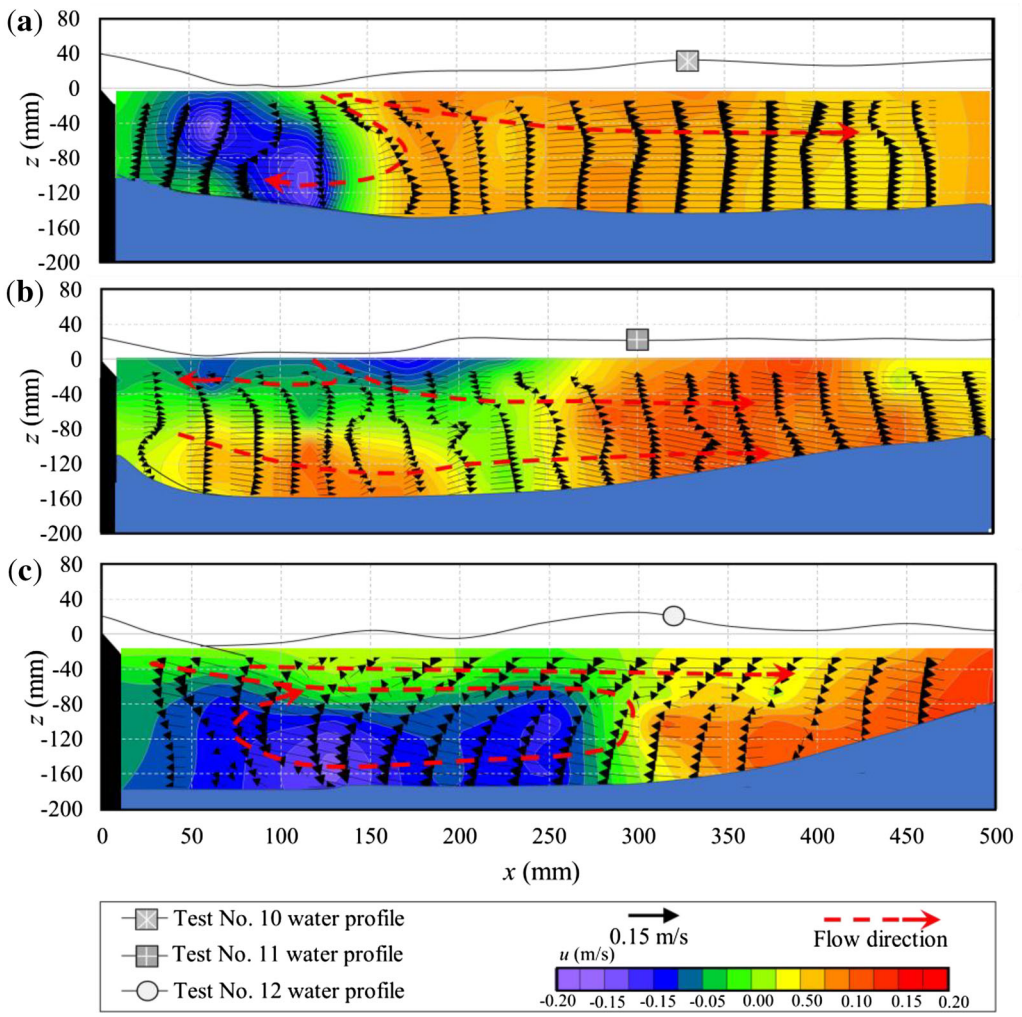

Figure 7. Flow regimes at the submerged weir; (a) Impinging regime of Model No. 10, (b) BSR (bed-surface regime), model No. 11, (c) Surface jump regime, model No. 12.

$$\frac{t}{h_o} = 1 - 0.126\lambda + 0.0076\lambda^2 - 0.00017\lambda^3, \ (R^2 = 0.96) \tag{4}$$

Also, for λ in range of zero to 15. λ is defined as $\lambda = \frac{\sqrt{gh_d}}{(\frac{q}{t}+z)}$ that q is discharge per unit width, g is gravitational acceleration, and h_d is the difference between upstream and downstream water level.

By considering these proposed boundaries, figure 5 was plotted to show the experimental data and developed proposed boundaries by considering the newly introduced regime (i.e., bed-surface regime). Also, Guan experiments were added in figure 5. These data were obtained due to $0<\lambda<0.8$. It seems that where $\lambda > 0.4$, a number of the surface wave Guan's experimental data exceeded to the regime between surface wave (SFR) and impinging jet regimes (IJR) which were developed as bed-surface regime (in figure 5 as BSR).

At this study, 24 experiments were plotted on Wu and Rajaratnam [2] boundaries in figure 5. The details of experiments have been presented in table 1. The vectors were plotted (2D- velocity profile at plane x-z) for a bed-surface regime based on Wu and Rajaratnam boundaries in figures 6, 7, 8 for Q_f =3.95, 6.49, 9.42, 17.7 L/s, respectively. As it can be seen in figure 6, due to t/h_o =0.36, 0.14 and -0.19 (Test Nos. 3, 4 and 5, respectively) the vector plots were plotted by Surfer 13 based on measured velocities by ADV. It indicates where t/h_o=0.36 the vector plots are divided as two directions. It is predicted that these samples were located on TR zone and the vector plots have a good agreement by TR regime which was proposed by Wu and and Rajaratnam [2]. Figure 6b) was plotted for another TR regime (i. e., t/h_o=0.14; Test No. 4). Although the vector plots were divided in two parts same as the earlier regime, it supposed that the bed-surface flow was developed near the bed-surface that the dash arrow shows this matter in figure 6b). The dash line shows the direction

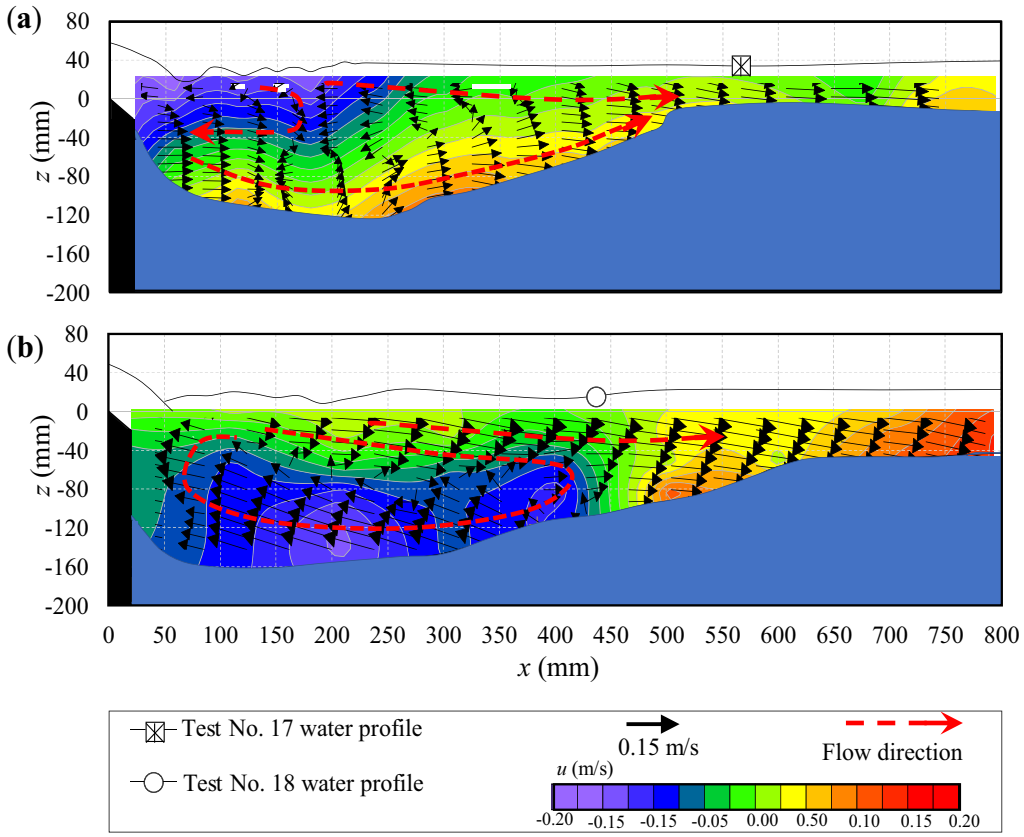

Figure 8. Flow regimes at the submerged weir; (a) BSR (sub-surface regime), model No. 4, (b) SJR, (Surface jump regime, model No. 5.).

of the currents which were deduced from velocity vectors. As it can be seen, due to the vertical profiles along a considered longitudinal section, the direction of the vectors (i.e., vectoral addition between stream-wise and vertical velocity) illustrate the orientation of the developed currents. By tracking the mentioned vectors, the general current (e.g., dash line can be plotted) can be specified. Also, the bed-surface flow is visible due to raising the flow discharge as in figures 8a) and b) and 9a). The vector plot in figure 6c) shows that the bed-surface flow developed near the bed was removed and a giant clock-wise vortex was located on the downstream the weir. It indicates that the plunged jet on downstream of SCW causes this clock-wise vortex that it can increase the intensity of the rotation at downstream of the sharp-crested weir. Also, this particular vector formation causes the maximum score hole shifted from downstream of SCW to near the weir location.

Figure 7 was plotted for t/h_o=0.33, 0.46 and 0.56 (e.g., test No. 12, 11 and 10). Figure 7a indicates on two directions of vectors which were separated from their orientations on this figure by two red colorued big arrows. By considering Wu and Rajaratnam boundary this test is located on TR zone (surface jump) that the shape of the water surface indicates this matter, too. Where the t/h_o is raised to 0.46 the flow pattern was switched to figure 7b. Comparison between figure 6b and b shows that the bed-surface flow was developed near the bed. It seems that the intensity of this pattern (presented as bed-surface regime) is directly dependent of the flow discharge. Also, the maximum scour hole depth was migrated at downstream of the weir position by increasing submergence ratio; however, by turning bed-surface regime to IJR, the maximum scour hole located to the downstream of SCW position. In addition, due to t/h_o=0.33 (see figure 6c), a giant clock-wise vortex was formed same as Test No.5 with this difference that this vortex has a larger rotational velocity. It is considered that the switching process of the maximum scour hole depth has a significant relation by this developed vortex. Hence, comparisons among Test No. 5, 12, 18 and 23 in figures 6c, 7c, 8b and 9b show a giant vortex at downstream the submerged weir, the maximum score hole location was developed near the weir location until it is located under the weir.

Figures 8 and 9 show vector plots for Q_f= 9.42,17.7 L/s, respectively. Although figure 8a (Test No. 17) is located on TR regime (Wu and Rajaratnam [2]), the bed-surface flow is still located near the bed elevation (e.g., the considered

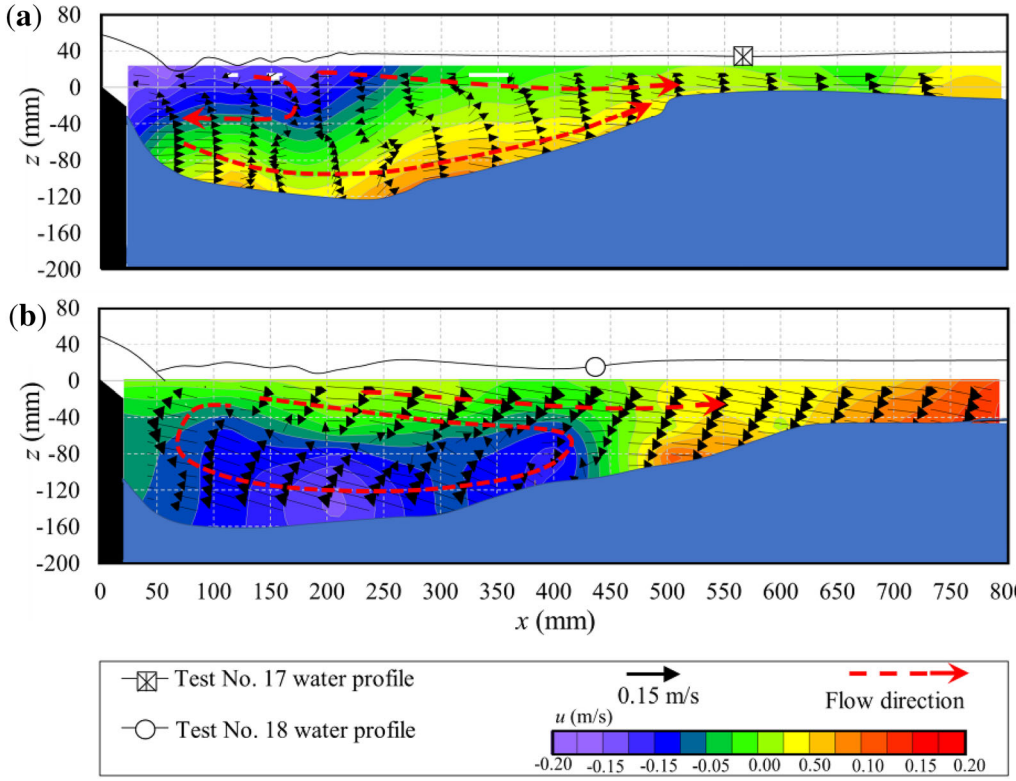

Figure 9. Flow regimes at the submerged weir; (a) SSR (sub-surface regime), model No. 22 and (b) SJR, (Surface jump regime), Model No. 23.

flow near the bed which were deduced from the vectoral addition of velocity components). This matter also has significance for Test No. 17 and 22 (figures 8a and 9a). Although the mentioned tests located into the TR zone, these did not have the TR regime flow pattern based on (Wu and Rajaratnam [2]). As a result, due to decreasing submerged ratio from 1 to less values, the flow pattern attains these regimes, SFR ((V) surface jet), then SFR ((IV) surface wave), TR ((III) surface jump), ((II) BSR bed-surface flow, IJR ((I)impinging jet). Therefore, based on hydraulic parameters, new BSR developed boundary was proposed as follows:

$$\frac{t}{h_o} = 1 - 0.1972\lambda + 0.0104\lambda^2 - 0.0008\lambda^3,\ (r^2 = 0.98),\ 0 < \lambda < 9.24 \quad (5)$$

4. Conclusions

1. Laboratory experiments were conducted to investigate the hydraulics and flow regimes of the submerged sharp-crested weirs. Due to different submergence ratio, the vector plots were depicted by Surfer 13 based on filtered velocity components. In total, the flow regimes were classified as (I) impinging jet, (II) sub-surface flow, (III) surface jump, (IV) surface wave, and (V) surface jet based on the vector plots of the flows [2, 7, 24]. Comparisons between vector plots shown between TR and IJR regimes, flow patterns were formed as another flow regimes which is not classified neither as IJR nor as TR regime. The experimental investigations show that the flow regimes due to special hydraulic condition located on another regime formation which is proposed as new regime, bed-surface regime (SSR).
2. In general, TR regime was defined as a condition which is occurred by a jump at the water surface and the velocity direction were divided into two wraps, one of them has upstream and another has a downstream orientation. Bydecreasing the submerged ratio, a bed-surface regime is formed near the bed that it can have a significant maximum scour hole position. When the experimental data were exceeded to IJR (Wu and Rajaratnam [2]) a great clockwise vortex was formed at downstream submerged sharp-crested weir. It is predicted that this vector formation causes that the position of maximum scour hole depth was switched to the upstream.
3. In present study, new equation was developed to show the boundary of bed-surface regime. An empirical equation was proposed to discriminate from bed-surface regime SSR zone at figure 5. As a result, the increase in the submerged ratio flow from free flow condition is seen. Flow patterns formed were: (I) impinging jet, (II)

ub-surface flow, (III) surface jump, (IV) surface wave, and (V) surface jet.

List of symbols

d_d	Downstream scour depth (m)
d_{dm}	Maximum downstream scour depth (m)
d_u	Initial upstream scour depth (m)
d_{50}	Mean diameter of sediment (mm)
g	Gravitational acceleration (m/s^2)
h	Upstream weir head (m)
h_{d}	Difference between upstream and downstream water level (m)
H	Upstream water level (m)
L	Scour hole length (m)
Q	Discharge (m^3/s)
t	Tail water (m)
u_{ave}	Averaged velocity (m/s)
u_{*c}	Critical shear velocity (m/s)
u_c	Critical threshold velocity (m/s)
x	Longitudinal direction
y	Transverse direction
z	Vertical direction
Z	Weir height (m)
ρ	Density of water (kg/m^3)

Data availability Some or all data, models, or code generated or used during the study are available from the corresponding author by request (data such as head-discharge and ADV measurements).

References

[1] Ackers P, White W R, Perkins J A and Harrison A J 1978 *Weirs and flumes for flow measurements*. Wiley, Chichester, UK 327

[2] Wu S and Rajaratnam N 1996 Submerged flow regimes of rectangular sharp-crested weirs. *ASCE. J. Hydr. Eng.* 122(7): 412–414

[3] Wu S and Rajaratnam N 1998 Impinging jet and surface flow regimes at drop. *IAHR. J. Hydr. Res.* 36(1): 69–74

[4] Azimi A H, Rajaratnam N and Zhu D Z 2014 Submerged flows over rectangular weirs of finite crest length. *ASCE. JID Eng.* 140(2): 148–160

[5] Azimi A H, Qian Y, Zhu D Z and Rajaratnam N 2015 An experimental study on circular slurry wall jets. *Int. J. Multiphase Flow.* 74: 34–44

[6] Azimi A H, Rajaratnam N and Zhu D Z 2016 Water surface characteristics of submerged rectangular sharp-crested weirs. *ASCE. J. Hydraul. Eng.* 142(5): 06016001–06016009

[7] Guan D, Melville B W and Friedrich H 2015 Live-bed scour at submerged weirs. *J. Hydraul. Eng.* 141(2): 04014071–04014112

[8] Skogerboe G V, Hyatt M L, Austin L H 1967 *Design and calibration of submerged open channel flow measurement structures: Part 4-weirs.* Utah Water Research Laboratory, Logan, Utah

[9] Rajaratnam N and Muralidhar D 1969 Flow below deeply submerged rectangular weirs. *J. Hydraul. Res.* 7(3): 355–374

[10] Ben Meftah M and Mossa M 2006 Scour holes downstream of bed sills in low-gradient channels. *J. Hydraul. Res.* 44(4): 497–509

[11] Bormann N E and Julien P Y 1991 Scour downstream of grade-control structures. *J. Hydraul. Eng.* 117(5): 579–594

[12] D'Agostino V and Ferro V 2004 Scour on alluvial bed downstream of grade-control structures. *J. Hydraul. Eng.* 130(1): 24–37

[13] Gaudio R, Marion A and Bovolin V 2000 Morphological effects of bed sills in degrading rivers. *J. Hydraul. Res.* 38(2): 89–96

[14] Melville B W and Friedrich H 2014 Flow patterns and turbulence structures in a scour hole downstream of a submerged weir. *ASCE J. Hydraul. Eng.* 140(1): 68–76

[15] Lenzi M A, Marion A and Comiti F 2003 Interference processes on scouring at bed sills. *Earth Surf. Process. Landforms.* 28(1): 99–110

[16] Lenzi M A, Marion A and Comiti F 2003 Local scouring at grade-control structures in alluvial mountain rivers. *Water Resour. Res.* 39(7): 1176

[17] Lenzi M A, Marion A, Comiti F and Gaudio R 2002 Local scouring in low and high gradient streams at bed sills. *J Hydraul. Res.* 40(6): 731–739

[18] Lu J Y, Hong J H, Chang K P and Lu T F 2012 Evolution of scouring process downstream of grade-control structures under steady and unsteady flows. *Hydrol. Process.* 27(19): 2699–2709

[19] Marion A, Lenzi M A and Comiti F 2004 Effect of sill spacing and sediment size grading on scouring at grade control structures. *Earth Surf. Process. Lancldforms.* 29(8): 983–993

[20] Marion A, Tregnaghi M and Tait S 2006 Sediment supply and local scouring at bed sills in high gradient streams. *Water Resour. Res.* 42(6): W06416

[21] Melville B W 1997 Pier and abutment scour: integrated approach. *ASCE. J. Hydraul. Eng.* 123(2): 125–136

[22] Pagliara S and Kurdistani S M 2013 Scour downstream of cross-vane structures. *J. Hydro-environ. Res.* 7(4): 236–242

[23] Scurlock S M, Thornton C I and Abt S R 2012 Equilibrium scour downstream of three-dimensional grade-control structures. *J. Hydraul. Eng.* 138(2): 167–176

[24] Guan D, Melville B W and Friedrich H 2014 Flow patterns and turbulence structures in a scour hole downstream of a submerged weir. *ASCE: J. Hydraul. Eng.* 140(1): 68–76

[25] Salehi S, Esmailli K and Azimi A H 2019 Mean velocity and turbulent characteristics of flow over half-cycle cosine sharp-crested weirs. *Flow Meas. Instrum.* 66: 99–110

[26] Wahl T L 2000 Analyzing ADV data using WinADV. *ASCE Proc. Joint Conf. on Water Resources Engineering and Water Resources Planning and Management*. Reston, VA. 10 p

[27] Salehi S and Azimi A H 2019 Discharge characteristics of weir-orifice and weir-gate structures. *J. Irrig. Drainage Eng.* 145(11): 04019025

[28] Salehi S, Azimi A H and Bonakdari H 2021 Hydraulics of sharp-crested weir culverts with downstream ramps in free-

flow partially, and fully submerged-flow conditions. *Irrig. Sci.* 39(2): 191–207

[29] Salehi S, Mostaani A and Azimi A H 2021 Experimental and numerical investigations of flow over and under weir-culverts with a downstream ramp. *J. Irrig. Drain. Eng.* 147(7): 04021029

[30] Salehi S and Azimi A H 2022 Effects of spoiler and piggyback on local scour under single and twin submerged pipes. *Ocean Eng.* 261: 112137

[31] Azimi A H and Salehi S 2022 Hydraulics of flow over full-cycle cosine and rectangular sharp-crested weirs. *Can. J. Civ. Eng.* 49(6): 954–968